5-25-2018

Isomers of Heteroleptic Derivatives of Nickel(II) Tris-Pyridinethiolate

Matthew McAllister Davis
Portland State University

Isomers of Heteroleptic Derivatives of Nickel(II) Tris-Pyridinethiolate

by

Matthew McAllister Davis

An undergraduate honors thesis submitted in partial fulfillment of the

requirements for the degree of

Bachelor of Science

in

University Honors

and

Chemistry

Thesis Adviser

Professor Theresa M. McCormick, Ph.D.

Portland State University

2018

Introduction

I. Solar Power & Artificial Photosynthesis

It is an observed fact that the earth has warmed significantly in the last century. Furthermore, there is an extremely strong scientific consensus that human behavior has contributed greatly to the changing climate.[1] Due to its large infrared cross-section and relatively high concentration, CO_2 is a large contributor to the greenhouse effect, itself a major contributor to climate change. Renewable sources of energy have showed strong promise for satiating the energy demands[2] of the United States without contributing to atmospheric CO_2. Renewable sources have risen to about 12% of United States energy usage in 2015[3]. Solar power is perhaps the best known of these options. However, despite the successes and proliferation of solar power, there are some limitations to conventional silicon solar panels. The issue that is the motivation for this thesis is the question of storage: power consumption does not follow the same pattern as the incoming power from the sun (irradiance), requiring some storage medium to supply power to the grid when the sun is not shining. Figure 1 demonstrates this fact with local data from the Portland area.

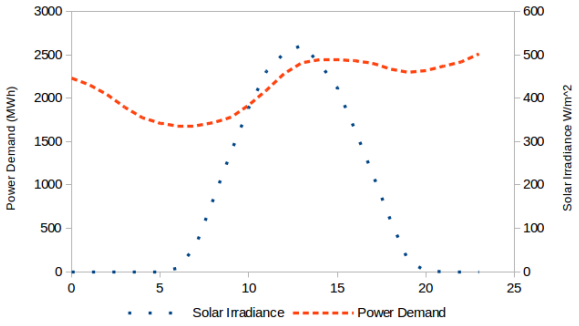

Figure 1: the average solar irradiance in Portland, OR from 2004 in the month of April and the power demand by hour in the PGE system on April 1st, 2018. Power demand data from U.S. Energy Information Administration.[4] Irradiance data from University of Oregon Solar Radiation Monitoring Laboratory.[5]

With very little storage capacity built in to the United States energy grid, the variability of renewable energy constitutes a major problem for incorporating renewables into our energy portfolio. Some of this deficit may be diminished by the energy production of wind and other renewable sources, however a renewable-only grid would require some form of power storage. There have been several proposals to remedy this issue. Perhaps the most well known is the implementation of a large chemical battery, either in a monolithic (one large battery) or distributed sense. Despite the attractiveness of such an approach, lithium-ion batteries produce a significant amount of waste. Recent

reports have recognized a growing problem of lithium ion battery disposal due to increased use in consumer electronics and electric vehicles without access to or incentive to use recycling services[6]. One alternative storage method is Artificial Photosynthesis (AP).[7,8] This process would use light energy to drive the water splitting reaction (Reaction 1) to from hydrogen gas (H_2) and oxygen gas (O_2) from liquid water. Water splitting is not generally achieved in a single step: the water splitting reaction is broken up into two half reactions, each mediated by a catalyst to increase the rate and efficiency of the reaction (Reaction 1a,b).

Reaction 1: Water splitting

$2H_2O_{(l)} + hv \rightarrow 2H_{2(g)} + O_{2(g)}$; $\Delta H = -286$ kJ/mol

a. $2H_2O \rightarrow O_{2\,(g)} + 4H^+_{(aq)} + 4e^-$

b. $4H^+_{(aq)} + 4e^- \rightarrow 2H_{2(g)}$

Reaction 1a is known as water oxidation and will not be focused on in this work. Reaction 1b is called proton reduction and forms the main focus of this thesis. Many systems have been found to catalyze this step, however none have been successful enough to make a profitable catalytic system. An ideal proton reduction catalyst would be fast, efficient, and robust.[8] These qualities are parameterized by turnover frequency (TOF), overpotential (η), and turnover number (TON), respectively. TOF is defined as the initial rate of reaction divided by the number of moles of catalyst. TOF is therefore the number of catalytic conversions per second per catalyst molecule. The overpotential is defined as the reduction potential minus the theoretical voltage of the reaction.

In this thesis, the system studied is the Nickel(II) tris-pyridinethiolate complex, which is covered in more detail in Section III of this introduction. This complex has primarily been studied as an electrocatalyst, but it has been shown that the findings of electrocatalytic studies can be translated into their photocatalytic counterparts.

III. A Brief Exploration of Nickel(II) Pyridinethiolate

Nickel(II) pyridinethiolate (Ni-pyt) (Figure 1) has been shown to produce hydrogen gas under photocatalytic conditions.[9] Studies of this complex and its derivatives have been a focus of this research group.[10,11] This complex is composed of a nickel center in the +2 oxidation state and three pyridinethiolate ligands (Figure 3).

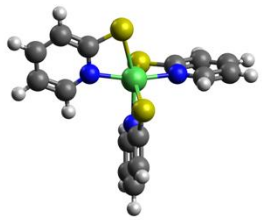

Figure 2: Nickel(II) pyridinethiolate viewed along the sulfur meridional plane. Geometry optimized at the M06-L/6-311+G* level of theory with a CPCM water solvation model. Calculation performed with Gaussian 09. [21]

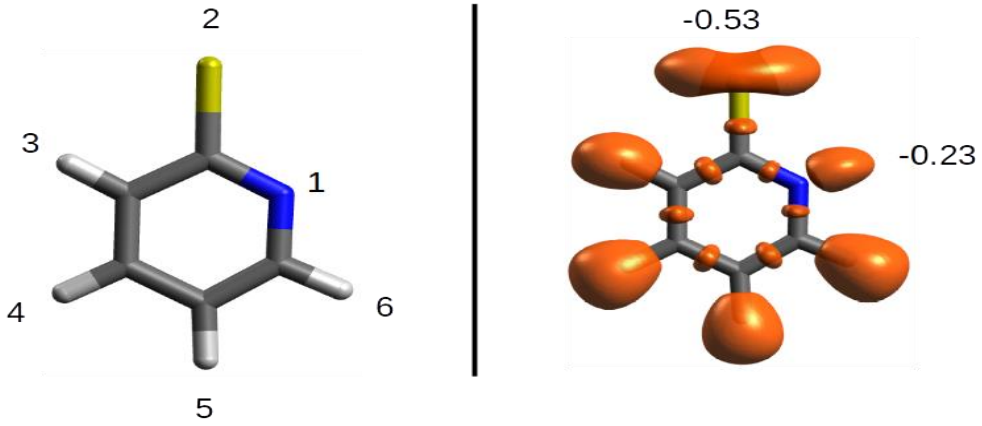

Figure 3: (left) Geometry of the pyridinethiolate ligand with IUPAC positions labeled. Geometry optimized at the HF/jun-cc-pvdz level of theory in the gas phase with Psi4 1.1.[13] (right) Electron Localization Function (ELF) (isovalue: 0.84) of the gas phase M05-2X Kohn-Sham wavefunction of the pyridinethiolate ligand. ELF generated with Multiwfn 3.5[14] and visualized with Avogadro. The ELF is interpreted as showing regions of paired electrons. Annotations are the Hirshfeld charges[15] calculated with Multiwfn.

Examining the gas phase electronic structure of pyridinethiolate provides a background for considering the reactivity of Ni-pyt and its derivatives. Figure 3 shows the electron localization function (ELF) for pyridinethiolate. The ELF shows regions of high electron localization, such as lone pairs or covalent bonds. For pyridinethiolate, the lone pairs on the S atom can be clearly seen and it is observed that the lone pairs lie more in the plane of the pyridine ring than in a tetrahedral configuration. The S atom can be assigned a sp^2 configuration with some double bond character between sulfur and the 2-position carbon. The lone pair on the nitrogen atom is directed outwards, consistent with an sp^2 configuration. Pyridinethiolate acts as a Lewis base by donating electron density from both the sulfur atom and the nitrogen atom (Figure 3) to form the distorted octahedral complex shown in Figure 2.

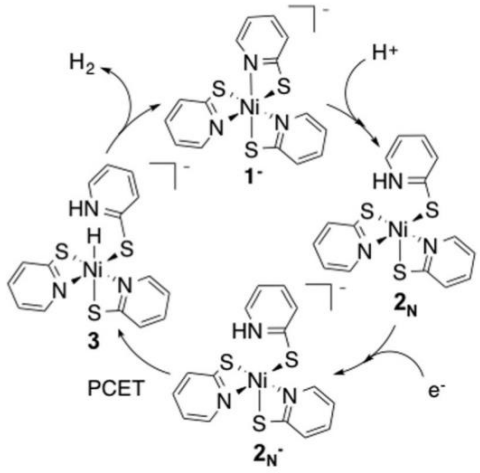

Figure 4: Literature proposed catalytic cycle of Ni-pyt.[10] Reprinted with permission.

Ni-pyt is thought to perform proton reduction through a four step catalytic cycle (Figure 4) in which the compound is protonated, then reduced, protonated once more, and finally reduced to form H_2. This mechanism is supported by experimental and computational evidence in the literature.[10]

IV. Approach to Substituent Modifications & Consequences of Homoleptic Modifications

A common approach to improving desirable qualities of a catalyst is substitution of the nonreacting groups to attempt to influence the chemistry of the reactive sites. Two common effects to exploit are so-called steric effects and electronic effects. Steric effects are the effect of nonbonding interactions between two groups, either intra- or inter-molecular. These are destabilizing interactions. Electronic effects are often classified into 'inductive' and 'resonance' effects. Inductive effects are a consequence of electronegativity differences in a molecule.

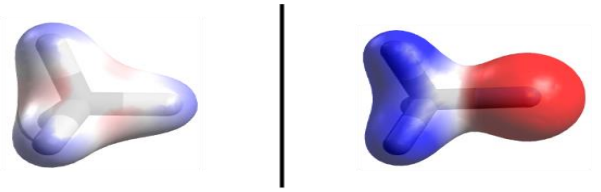

Figure 5: Electron density isosurface (isovalue=0.08) of methane (left) and fluoromethane (right) colored by total electrostatic potential.

Looking at the electrostatic potential maps of methane and fluoromethane in Figure 5, it is clear that the hydrogen atoms in fluoromethane are more electropositive than the hydrogen atoms in methane. This is attributable to the increased Pauling electronegativity of fluorine (4.0) than hydrogen (2.2). The same effect can be used to withdraw or donate electron density from a reacting group. For example, trifluoroacetic acid is much more acidic than acetic acid due to the inductive effect of the fluorine atoms that stabilize the negatively charged conjugate base.

IV. Isomers of Meridional Tris-chelate Complexes

For a catalyst involved in the proton reduction half-reaction of artificial photosynthesis, pK_a and reduction potential (E°) are key parameters for a successful catalyst.[8,1618] Unsymmetric bidentate ligands with chemically nonequivalent donor atoms are common in coordination chemistry; even simple substitutions to the structure effects the reactivity of the resulting complex and has a strong connection to the nature of the donor atoms in the ligand. In an octahedral complex with stoichiometry ML_3 where L is a bidentate ligand the *fac* or *mer* isomer can be formed. In many complexes there is an enthalpic preference for either the *mer* or *fac* isomer, however due to the 3:1 statistical ratio between the *mer* and *fac* isomers, the *mer* isomer is frequently formed in significant quantities due to entropic effects.[19] It has been identified that the *fac* isomer is more favorable when there is a larger difference in the σ-donor and π-accepting character of the donor atoms.[19] For unsymmetrical chelates the *mer* isomer has an interesting property in that even in a homoleptic complex all ligands are chemically inequivalent due to the lack of axes of rotation or mirror planes. This property of these complexes has not been thoroughly investigated. Substitution of one chelate with another ligand forms a heteroleptic complex, ML_2L' where L' is the substituted ligand. This introduces further complexities to the isomerism of the complex. Due to the lack of axes or planes of symmetry, in this complex there are now three unique *mer* isomers and a single *fac* isomer.

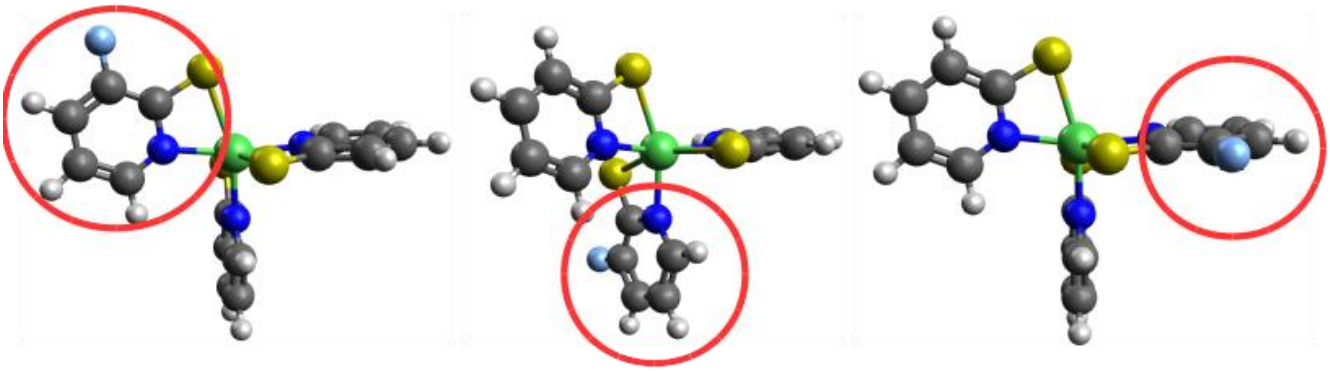

Figure 6: The three isomers ([L],[C],[R]) of Nickel(II) bis-2-mercaptopyridine 2-mercapto-3-fluoropyridine viewed along the sulfur meridional plane. The [C] isomer has been rotated slightly for ease of locating the unique ligand.

While studying the properties of heteroleptic derivatives of Ni-pyt, it was realized that the different isomers of heteroleptic complexes may be important in understanding the effect of heteroleptic derivatives on catalyst properties. In this thesis I propose, on the basis of quantum chemical calculations, a relationship between binding site preference ([L], [C], or [R] isomer) and the nature of the unique ligand in nickel(II) tris-2-mercaptopyridine derivatives such as those shown in Figure 1. Furthermore, I show that the isomers of these complexes can have different reactivity that could be leveraged as a way to tune octahedral ML_3 complexes with a preference for the meridional isomer.

Methods

The free energies of the three isomers (see *Isomer Nomenclature* for an explanation of these isomers) were calculated with density functional theory (DFT). This popular method is one of the most accurate quantum chemical tools to apply to systems of the size and complexity of Ni-pyt.

Ligand Modifications

To elucidate the relationship between binding site preference and the nature of the unique ligand in a heteroleptic complex, eight substituent groups were selected. These are methyl ($-CH_3$), amino ($-NH_2$), hydroxy (-OH), methoxy ($-OCH_3$), cyano (-CN), chloro (-Cl), and fluoro (-F). These substituents were placed in the 3, 4, 5, and 6 positions of the 2-mercaptopyridine ligand (Figure 2).Thus, a total of 28 unique ligands were explored.

Theoretical Approach

Density functional theory (DFT) was used to compute structures, properties, and energies of the coordination complexes explored. For the coordination complexes, the M06-L functional was employed due to its ability to adequately capture both main group and metal-ligand chemistry.[20] For the investigation of the electronic properties of the ligands, Moller-Plesset perturbation theory at second order (MP2) was used.

Isomer Nomenclature

In a 2:1 parent to modified ligand ratio, the unique ligand will occupy one site on the coordination complex, forming one of three isomers. A unique naming scheme was needed for the isomers of the complexes investigated. It was decided that the simplest scheme is obtained by the following description (visually described in Figure 7: When viewing the complex along the meridional plane defined by the three sulfur atoms with the sulfurs making an upwards pointing 'V', and with the vertically oriented ligand on the left, the unique ligand is declared either the '[R]', '[C]', or '[L]' isomer. The letters stand for 'right', 'center', and 'left', respectively. The brackets help to clarify between other types of isomers, e.g. R & S isomers, D & L isomers, and this type.

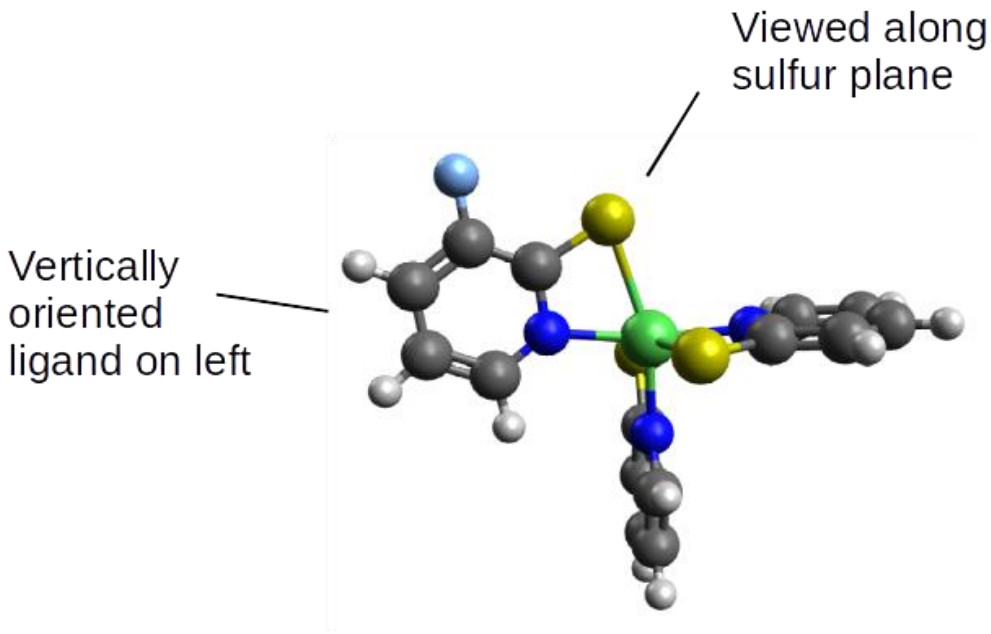

Figure 7: Visual description of the naming scheme for [R], [C], and [L] isomers showing the [L] isomer of the 3-fluoro substituted heteroleptic complex.

Computational Details

Geometries of all coordination complexes were optimized with the M06-L functional[20] and 6-311+G(d) basis set. A polarizable continuum model for water was used for dielectric solvent effects. Explicit solvation was not incorporated. Free ligands were optimized in the gas phase at the MP2/jun-cc-pvtz level of theory. Geometry optimizations and frequency calculations for all coordination compounds were performed with Gaussian 09.[21] Single point calculations used for obtaining condensed Fukui function values were performed with Psi4 1.1.[13] Multiwfn 3.4.1[14] was used for obtaining Hirshfeld charges, ELF maps, electrostatic potential maps, and for AIM analysis.

Results & Discussion

The probability of the occupation of a particular site can be calculated by comparing the computed free energies of the isomers. In some cases, a preference for one isomer over the others is found.

Indirect Control: Electronic effects in the 3, 4, and 5 positions

Substitutions on the 3, 4, and 5 positions do not significantly interact with other ligands or with the nickel center. These positions will be described as the 'indirect' positions hereafter. The isomer preference shown, if any, must correspond to purely electronic effects. The probabilities, based on a Boltzmann distribution of the free energies, of the isomers of the indirect substitutions are shown in Table 1.

Table 1. Normalized isomer populations for 3- substituted ligands. P([X]) is the normalized population of isomer [X].

GROUP	P([L])	P([C])	P([R])
CH_3	0.258	0.345	0.397
Cl	0.25	0.337	0.412
CN	0.239	0.350	0.412
F	0.346	0.228	0.425
CH_2OH	---	---	---
NH_2	0.332	0.264	0.404
OH	---	---	---

Table 2. Normalized isomer populations for 4-substituted ligands. P([X]) is the normalized population of isomer [X].

GROUP	P([L])	P([C])	P([R])
CH_3	0.391	0.293	0.316
Cl	0.279	0.277	0.443
CN	0.400	0.262	0.337
F	0.443	0.259	0.298
CH_2OH	0.409	0.299	0.292
NH_2	0.473	0.209	0.319
OH	0.484	0.318	0.199

Table 3. Normalized isomer populations for 5-substituted ligands. P([X]) is the normalized population of isomer [X].

GROUP	P([L])	P([C])	P([R])
CH_3	0.353	0.398	0.295
Cl	0.299	0.440	0.259
CN	0.259	0.388	0.378

F	0.237	0.473	0.307
CH_2OH	0.197	0.406	0.354
NH_2	0.271	0.42	0.326
OH	0.236	0.351	0.351

With the exception of two missing data points (CH_2OH in the 2-position and OH in the 2-position), the isomer preferences are only slight for these complexes. Furthermore, no convincing relationship between isomer preferences and electronic parameters of the modified ligands is discovered. Figure 1 shows the lack of relationship between the Hammett constant σ(m) and the probabilities of the isomers for the 4-substituents.

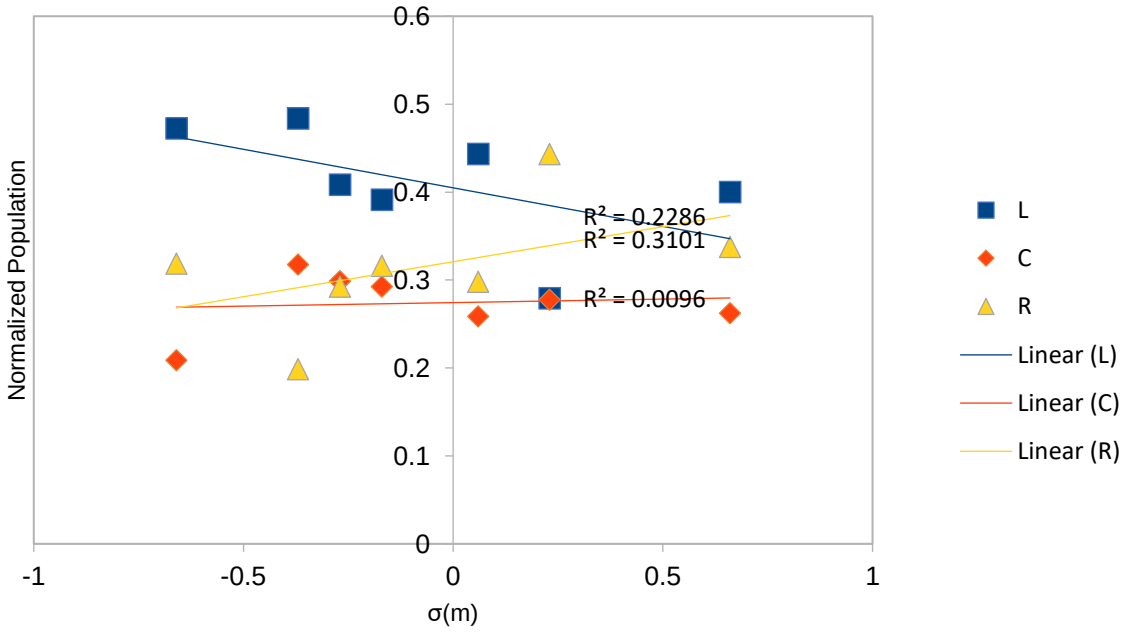

Figure 1: Graph of Boltzmann probability versus Hammett constant σ(m) for 4-substituents.

The position of the 4-substitutions are not special; for the 3, 4, and 5 substitutions no trend is discovered for the electron withdrawing nature of the substituent and the distribution of isomers. These results indicate that there is little control of isomer preference through the electronic structure of the unique ligand. It is more likely that these differences, which mostly lie in the 1-3 kcal/mol range, will be swamped by explicit solvation effects and little to no preference would be observed.

Direct Control: the 6- substitution

However, the 6- position is unique: the substituents in this position have the ability to interact directly with the other ligands. This is best displayed by viewing an example.

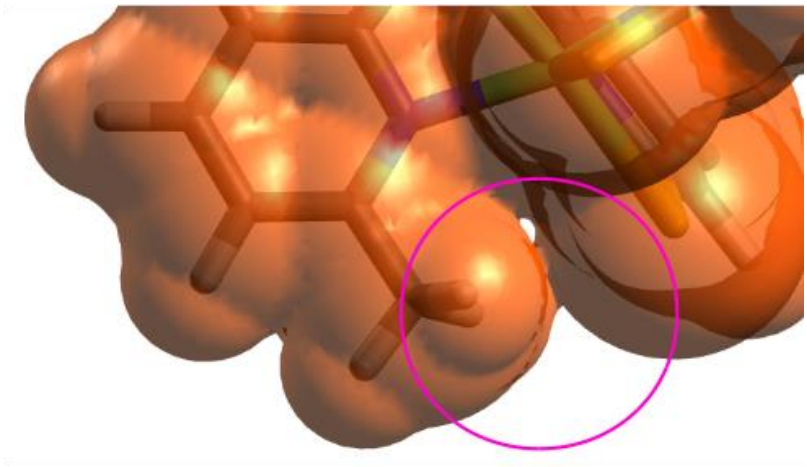

Figure 2. Contact of the Van der Waals spheres of the -CH_3 in the 6-position of the right ligand and the sulfur atom of the center ligand.

This makes it possible to use direct ligand-ligand interactions to stabilize or destabilize the molecule. To destabilize a position, a group can be introduced that has steric interactions (as shown in Figure 2) with another ligand. However, the 6-position on the left ligand is much less sterically hindered than the center or right ligands as it is pointing into a nitrogen atom, whereas on the right and center the 6- position is pointing into the much larger sulfur atom. This is reflected in the computed proabilities: Table 4 shows the isomer preferences in the 6- positions.

Table 4. Isomer preferences for 6-substituted ligands. P([X]) is the probability of isomer [X]

GROUP	P([L])	P([C])	P([R])
CH_3	0.353	0.398	0.295

Cl	0.299	0.44	0.259
CN	0.259	0.388	0.378
F	0.237	0.473	0.307
CH_2OH	0.197	0.406	0.354
NH_2	0.271	0.42	0.326
OH	0.236	0.351	0.351

For the sterically hindered groups, such as $-CH_3$, -Cl, -CN, and -F, the [L] isomer is much more favorable than the [C] or [R] isomers. However, two groups stand out as exceptions to this rule: the $-NH_2$ and -OH groups have the reversed trend: they are much more favorable for the [C] and [R] isomers. Inspecting the equilibrium structures provides an explanation in terms of hydrogen bonding.

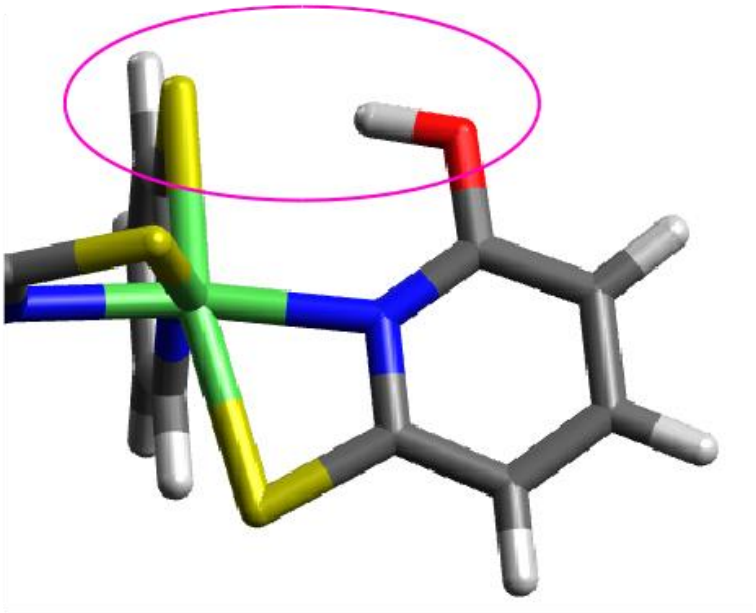

Figure 3. Hydrogen bonding between the hydroxyl group on the 6-position of the right ligand with the sulfur atom of the center ligand.

The right ligand (Figure 3) and center ligand will form this hydrogen bond to a polarizable sulfur atom, whereas the left ligand will form only a weak hydrogen bond to the nitrogen atom of the center ligand, a much worse hydrogen bond acceptor. This is reflected in the Boltzmann probabilities of the substitutions (Table 4). The hydrogen bond (HB) donor substitutions ($-NH_2$ and -OH) behave slightly differently, with the -OH substitution favoring the [C] isomer slightly over the [R], whereas $-NH_2$ favors both roughly equally. Furthermore, $-NH_2$ is less selective, with P([L]) = 0.095 compared to 0.004 for the -OH substituted ligand. This can be explained in terms of HB enthalpies

by estimating the strength of the HB through a linear fit of hydrogen bond enthalpy against electron density at the HB bond critical point: [22]

$$E(\rho) = -6.6(8.0) + 1215(440)\rho \ (e/a_o^3)$$

[1]

with standard deviations in parentheses.

Table 5. Electron densities at the hydrogen bond critical point and hydrogen bond energies estimated with Equation 1* for intraligand hydrogen bonding.

R=	Isomer	ρ (e/a_o^3)	E (kcal/mol)
OH	[R]	2.85E-02	6.711
	[L]	1.86E-02	3.82
	[C]	2.93E-02	6.944
NH_2	[R]	1.92E-02	3.986
	[L]	1.34E-02	2.327
	[C]	1.95E-02	4.082

The values in Table 5 attribute the preference of [R] and [C] isomers to the strength of the hydrogen bonds. The difference in free energies of the isomers follows the same trend, although the differences in hydrogen bond energies are slightly higher than the differences in free energy.

In summary up to this point, the 3, 4, and 5 positions provide only weak selectivity for isomer preference, and are unlikely to exert sufficient selectivity to provide synthetic control over the isomer formed. However, due to direct ligand-ligand interactions, the substitutions on the 6-positions have a much stronger effect, often resulting in

computed 70-80% isomer preferences assuming thermodynamic reaction control. The control with hydrogen bonding is particularly interesting, as it may allow greater control of the reactivity of the complex.

Application to Catalyst Design

At this point, some degree of isomer selectivity is predicted using intramolecular interactions, either hydrogen bonding (favoring [R] and [C]) and steric (favoring [L]). Furthermore, one of the original motivations for this work was to control the site of protonation such that an EDG can be placed in that position, with either neutral or EWG ligands in the other positions. Therefore, I propose the following complex as an improved proton reduction catalyst:

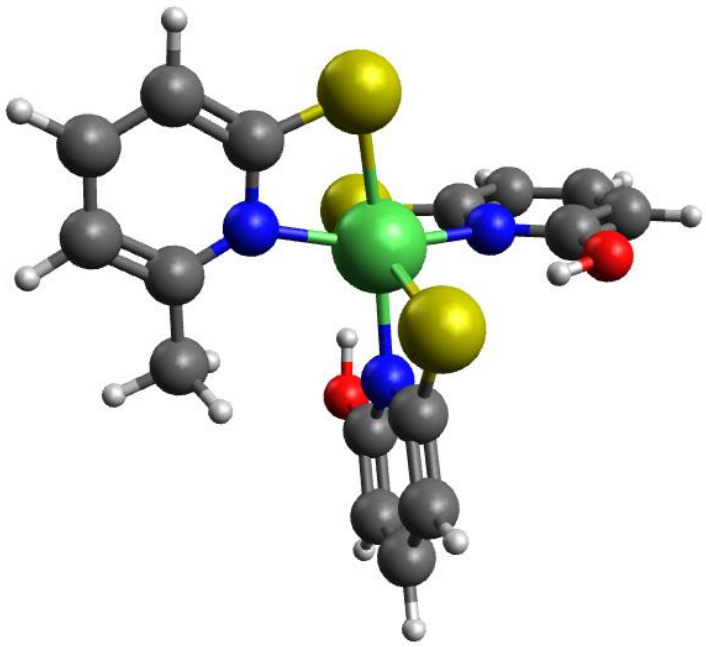

Figure 4: Proposed catalyst. A derivative of Ni-pyt with two 6-hydroxy and a single 6-methyl substituted pyridinethiolate ligand.

The 6-hydroxy ligands act as both hydrogen bond donors and acceptors, forming a linkage with a combined HB energy of ~14 kcal/mol by the previous approximation. From the previous results, this is predicted to preferentially place the 6-hydroxy ligands in the R and C positions, and to reduce the tendency of the R and C ligands to dechelate. Furthermore, steric interactions provides a thermodynamic incentive for the 6-methyl substituted ligand to occupy the L site, and to provide greater tendency of the L site to dechelate and initiate the catalytic cycle. The combination of these effects is predicted to provide near quantitative formation of the arrangement above: The isomer shown in Figure 4 is calculated to be formed with 99.8% yield in the thermodynamic limit. Furthermore, it is nearly certain that the protonation step would occur on the L ligand while the other two ligands remain inert. This allows several

benefits. The ligand with the 6-methyl group can be further modified to provide additional EDG character, or even derivatives with a chromophore that could reduce the pyridinium proton into a hydrogen radical in the presence of a sacrificial electron donor. The 6-hydroxyl ligands could also (or alternatively) be derivatized with electronic influencing groups or a chromophore that is able to reduce the nickel center in the presence of a sacrificial electron donor, such that the hydride intermediate could be formed. Other complexes can also be derivatized in such a manner, however knowing which ligand will be protonated and which will remain chelated allows much greater tunability of the complex. Thus, the complex proposed can be used as a well characterized model system for heteroleptic complexes. The rigidity of the complex due to the hydrogen bonding network also indicates that ligand rearrangement, if it occurs at all, will be further reduced. This means that the hydride intermediate will form in the coordination site previously occupied by the pyridyl nitrogen of the L ligand. This offers the benefit of prearrangement of the transition state just prior to hydrogen release, in which the hydride and the pyridinium nitrogen meet to form free hydrogen, which may increase the turnover frequency of the catalyst. The hydrogen bonding network also reduces electron density on the S atoms, which could reduce the reduction potential for the nickel center, as it will be more oxidized as electron density is withdrawn from its ligands.

Conclusion

In this thesis, the existence and consequences of heteroleptic isomers in the Ni-pyt proton reduction catalyst were explored. Eight substituents in four ring positions on pyridinethiolate were examined. Comparison of the Gibbs free energies of the isomers showed a lack of any isomer preference for ligands with 3, 4, and 5 position modifications. However, in the 6 position, intramolecular interactions come into play and offer a pathway to isomeric selectivity. For $–CH_3$, -Cl, -F, and –CN the steric interactions are much greater in the Center and Right positions, due to an imposing sulfur atom. In the Left position, the steric consequences of adding such a group is less, as only a nitrogen atom is present to interact. For –OH and $–NH_2$ the reverse selectivity was observed. In this case, this was due to the difference in hydrogen bond energies. A hydrogen bond with nitrogen as an acceptor was shown to be much less favorable than with a sulfur as the acceptor, thus favoring the Center and Right positions. The strength of these selectivities was reinforced by computing the isomer preference for a catalyst with two hydroxyl and one methyl group in the 6 positions, with a nearly 100% preference for the methyl group in the left position.

References

1. Climate change evidence: How do we know? Climate Change: Vital Signs of the Planet Available at: https://climate.nasa.gov/evidence. (Accessed: 17th April 2018)
2. Energy use (kg of oil equivalent per capita) | Data. Available at: https://data.worldbank.org/indicator/EG.USE.PCAP.KG.OE?locations=US. (Accessed: 17th April 2018)
3. Alternative and nuclear energy (% of total energy use) | Data. Available at: https://data.worldbank.org/indicator/EG.USE.COMM.CL.ZS?locations=US. (Accessed: 17th April 2018)
4. U.S. Electric System Operating Data. Available at: https://www.eia.gov/realtime_grid/#/data/graphs?end=20180409T17&start=20180402T21&bas=0000000000002&regions=
5. UO SRML stations: Portland, OR. Available at: http://solardat.uoregon.edu/Portland.html. (Accessed: 9th April 2018)
6. Zeng, X., Li, J. & Liu, L. Solving spent lithium-ion battery problems in China: Opportunities and challenges. *Renew. Sustain. Energy Rev.* **52,** 17591767 (2015).

7. Han, Z. & Eisenberg, R. Fuel from Water: The Photochemical Generation of Hydrogen from Water. *Acc. Chem. Res.* **47,** 25372544 (2014).

8. Eckenhoff, W. T. & Eisenberg, R. Molecular systems for light driven hydrogen production. *Dalton Trans.* **41,** 13004 (2012).

9. Han, Z., Shen, L., Brennessel, W. W., Holland, P. L. & Eisenberg, R. Nickel Pyridinethiolate Complexes as Catalysts for the Light-Driven Production of Hydrogen from Aqueous Solutions in Noble-Metal-Free Systems. *J. Am. Chem. Soc.* **135,** 1465914669 (2013).

10. N. Virca, C. & M. McCormick, T. DFT analysis into the intermediates of nickel pyridinethiolate catalysed proton reduction. *Dalton Trans.***44,** 1433314340 (2015).

11. Virca, C. N., Lohmolder, J. R., Tsang, J. B., Davis, M. M. & McCormick, T. M. Effect of Ligand Modification on the Mechanism of Electrocatalytic Hydrogen Production by Ni(pyridinethiolate)3 Derivatives. *J. Phys. Chem. A* (2018). doi:10.1021/acs.jpca.7b11912

12. Valiev, M. *et al.* NWChem: A comprehensive and scalable open-source solution for large scale molecular simulations. *Comput. Phys. Commun.***181,** 14771489 (2010).

13. Parrish, R. M. *et al.* Psi4 1.1: An Open-Source Electronic Structure Program Emphasizing Automation, Advanced Libraries, and Interoperability. *J. Chem. Theory Comput.***13,** 31853197 (2017).

14. Lu Tian & Chen Feiwu. Multiwfn: A multifunctional wavefunction analyzer. *J. Comput. Chem.***33,** 580592 (2011).

15. Hirshfeld, F. Bonded-atom fragments for describing molecular charge densities. *Theor. Chim. Acta***44,** 129138 (1977).

16. Das, A., Han, Z., Brennessel, W. W., Holland, P. L. & Eisenberg, R. Nickel Complexes for Robust Light-Driven and Electrocatalytic Hydrogen Production from Water. *ACS Catal.***5,** 13971406 (2015).

17. Solis, B. H. & Hammes-Schiffer, S. Theoretical Analysis of Mechanistic Pathways for Hydrogen Evolution Catalyzed by Cobaloximes. *Inorg. Chem.***50,** 1125211262 (2011).

18. Virca, C. N., Lohmolder, J. R., Tsang, J. B., Davis, M. M. & McCormick, T. M. Effect of Ligand Modification on the Mechanism of Electrocatalytic Hydrogen Production by Ni(pyridinethiolate)3 Derivatives. *J. Phys. Chem. A* (2018). doi:10.1021/acs.jpca.7b11912

19. Dabb, S. L. & Fletcher, N. C. mer and fac isomerism in tris chelate diimine metal complexes. *Dalton Trans.***44,** 44064422 (2015).

20. Zhao, Y. & Truhlar, D. G. The M06 suite of density functionals for main group thermochemistry, thermochemical kinetics, noncovalent interactions, excited states, and transition elements: two new functionals and systematic testing of four M06-class functionals and 12 other functionals. *Theor. Chem. Acc.***120,** 215241 (2008).

21. Gaussian 09, Revision A.02, M. J. Frisch, G. W. Trucks, H. B. Schlegel, G. E. Scuseria, M. A. Robb, J. R. Cheeseman, G. Scalmani, V. Barone, G. A. Petersson, H. Nakatsuji, X. Li, M. Caricato, A. Marenich, J. Bloino, B. G. Janesko, R. Gomperts, B. Mennucci, H. P. Hratchian, J. V. Ortiz, A. F. Izmaylov, J. L. Sonnenberg, D. Williams-Young, F. Ding, F. Lipparini, F. Egidi, J. Goings, B. Peng, A. Petrone, T. Henderson, D. Ranasinghe, V. G. Zakrzewski, J. Gao, N. Rega, G. Zheng, W. Liang, M. Hada, M. Ehara, K. Toyota, R. Fukuda, J. Hasegawa, M. Ishida, T. Nakajima, Y. Honda, O. Kitao, H. Nakai, T. Vreven, K. Throssell, J. A. Montgomery, Jr., J. E. Peralta, F. Ogliaro, M. Bearpark, J. J. Heyd, E. Brothers, K. N. Kudin, V. N. Staroverov, T. Keith, R. Kobayashi, J. Normand, K. Raghavachari, A. Rendell, J. C. Burant, S. S. Iyengar, J. Tomasi, M. Cossi, J. M. Millam, M. Klene, C. Adamo, R. Cammi, J. W. Ochterski, R. L. Martin, K. Morokuma, O. Farkas, J. B. Foresman, and D. J. Fox, Gaussian, Inc., Wallingford CT, 2016.

22. Rozenberg, M. “The Hydrogen Bond – Practice and QTAIM Theory.” *RSC Adv.*, vol. 4, no. 51, 2014, pp. 26928–26931., doi:10.1039/c4ra03889d.